SPECIAL SECTION

Efficacy of modal curvature damage detection in various pre-damage data assumptions and modal identification techniques

Milena DROZDOWSKA[1] [*], **Marek SZAFRAŃSKI**[2] , **Anna SZAFRAŃSKA**[3] ,
and **Agnieszka TOMASZEWSKA**[1]

[1] Department of Structural Mechanics, Faculty of Civil and Environmental Engineering,
[2] Department of Engineering Structures, Faculty of Civil and Environmental Engineering,
[3] Division of Differential Equations and Applications of Mathematics, Institute of Applied Mathematics
Gdańsk University of Technology, Narutowicza 11/12, 80-233, Gdańsk, Poland

Abstract. The efficacy of modal curvature approach for damage localization is discussed in the paper in the context of input data. Three modal identification methods, i.e., Eigensystem Realization Algorithm (ERA), Natural Excitation Technique with ERA (NExT-ERA) and Covariance Driven Stochastic Subspace Identification (SSI-Cov), and four methods of determining baseline data, i.e., real measurement of the undamaged state, analytical function, Finite Element (FE) model and approximation of current experimental mode shape, are considered. Practical conclusions are formulated based on analysis of two cases. The first is a laboratory beam with a notch and the second is a stone-masonry historic lighthouse with modern restoration in its upper part. The analysis shows that NExT-ERA and SSI-Cov in combination with approximation of current mode shape provide high efficacy in damage localization alongside relatively straightforward determination of baseline data. It proves that the construction of advanced FE models of a structure can be replaced with a much simpler method of baseline data acquisition. Furthermore, the research shows the structural mode shapes identified with ERA may not always indicate the presence of damage.

Keywords: modal curvature based damage detection; stochastic subspace identification; eigensystem realization algorithm; natural excitation technique; masonry tower.

1. INTRODUCTION

Vibration-based structural health monitoring (VBSHM) comprises many techniques that are applied in analysis of mechanical, civil and also biological objects. They allow us to study structural health or structural mechanical behaviour with local or global perspective, on the basis of measured vibration signals [1]. Nondestructiveness and ease of data measuring are assets of VBSHM, thus there are many applications in existing building structures, primarily in bridges [2–4], but also in historic structures, particularly in masonry or rock towers [5–7].

Damage detection and localization is a big category of VBSHM problems. They rely on analysis of vibration signal time-series or modal data identified from the vibration response. Some group of methods has the additional advantage of not requiring baseline data. For example, the traveling ultrasonic waves technique enables detection and localization of damage using only current measurements, as proved in [8] in the context of crack detection in concrete elements. However, the method is suitable only for structural members. On the other hand wavelet analysis or fractal dimension-based crack detector reveal high

effectiveness in damage localization or even estimation of its size [9, 10]. Since they usually are used to detect anomalies in mode shapes, they have potential to provide global analysis of the entire structure.

High efficacy reveals also methods formulated on a basis of mode shape curvature. The pioneer formulation is presented in [11] and its further modifications are proposed in [12, 13]. There are numbers of practical applications of modal curvature method involving structural members, such as beams [14], plates [15], masonry walls [16] or bridges [17].

The paper presents an analysis of the modal curvature-based damage localization efficacy related to different ways of determining baseline data and identifying mode shapes. A pioneer formulation is considered, which assumes that the bending stiffness at the location of the damage is reduced, leading to local change of the mode curvature. Four strategies for determining baseline data are considered: real measurement of the undamaged structure, analytical function, finite element model-based and approximation of current experimental mode shape. While all of them are applicable to cases of laboratory models or newly built structures, only the last two strategies can be used in cases of existing structures. In order to determine the mode shapes of the identified structures, three modal identification (MID) methods are used, namely Eigensystem Realization Algorithm, Natural Excitation Technique with ERA and Covariance Driven

---
[*]e-mail: milena.drozdowska@pg.edu.pl

M. Drozdowska, M. Szafrański, A. Szafrańska, and A. Tomaszewska

Stochastic Subspace Identification. The analysis focuses on two objects: a laboratory beam with a notch, and on a historic masonry lighthouse with modern restoration in its upper part.

2. MATERIALS AND METHODS

2.1. Modal curvature approach to damage detection

In the adopted methodology [11], the mode shape curvature is determined as the second derivative of mode shape and for a discrete function can be calculated using the central difference method. The curvature $C_j(i)$ of j-th mode ϕ_j at the location i, for irregularly distributed points, as in practical cases, is defined as

$$C_j(i) = \frac{\phi_j(i+1) - 2\phi_j + \phi_j(i-1)}{0.5(L_{i+1}^2 + L_{i-1}^2)}, \quad (1)$$

where L_{i+1} and L_{i-1} are distances between measurement points $i+1$ and i, or respectively i and $i-1$. The mode shape curvature damage index takes form

$$W_{C_j}(i) = |C_j^a(i) - C_j^0(i)|, \quad (2)$$

where C_j^a and C_j^0 denotes the curvature of mode shape identified for the structure in the actual state and in the reference state, respectively. The normalized damage index $Z_C(i)$, which provides information about the probability of damage occurrence in section i, is defined by

$$Z_C(i) = \frac{W_C(i) - \bar{W}_C}{\sigma_C}, \quad (3)$$

where $\bar{W}_C$ is the mean value of $W_C(i)$, while σ_C is the standard deviation of the index. From the normal distribution of the index $W_C(i)$, if the likelihood of result $Z_C(i)$ equals 2, there is 97.725% confidence, that the damage is located at i-th point.

2.2. Modal identification methods

2.2.1. Eigensystem Realization Algorithm (ERA)

The ERA was developed as the evolution of the Ho-Kalmann minimum realization problem [18] and estimates the modal parameters, i.e., frequencies, damping ratios and mode shapes, based on finite-time and noisy experimental data [19, 20]. The basic principle of the ERA involves the identification of system matrices $\mathbf{A}_{n \times n}$, $\mathbf{B}_{n \times p}$ and $\mathbf{C}_{p \times n}$ of a state-space model:

$$\begin{aligned} \mathbf{x}_{k+1} &= \mathbf{A}\mathbf{x}_k + \mathbf{B}\mathbf{u}_k, \\ \mathbf{y}_k &= \mathbf{C}\mathbf{x}_k, \end{aligned} \quad (4)$$

which represents the discrete-time, linear time-invariant (LTI) system of order n (n is the number of significant equations to define the identified system and p is the number of sensors). The algorithm starts from forming Hankel matrix based on the measured Markov parameters $\mathbf{y}_k = [y_{k,1}, y_{k,2}, \ldots, y_{k,p}]^T$, i.e., the vectors that are composed of the free-vibration responses at

k-th time step in each sensor:

$$\underset{(\alpha p \times \beta)}{\mathbf{H}}(k-1) = \begin{bmatrix} \mathbf{y}_k & \mathbf{y}_{k+1} & \cdots & \mathbf{y}_{k+\beta-1} \\ \mathbf{y}_{k+1} & \mathbf{y}_{k+2} & \cdots & \mathbf{y}_{k+\beta} \\ \mathbf{y}_{k+2} & \mathbf{y}_{k+3} & \cdots & \mathbf{y}_{k+\beta+1} \\ \vdots & \vdots & \ddots & \vdots \\ \mathbf{y}_{k+\alpha-1} & \mathbf{y}_{k+\beta} & \cdots & \mathbf{y}_{k+\alpha+\beta-2} \end{bmatrix}. \quad (5)$$

The method parameters α and β decide about the size of the Hankel matrix, i.e. number of signal samples used. The algorithm results in the minimum realization defined by the triple:

$$\begin{aligned} \hat{\mathbf{A}} &= \mathbf{S}_n^{-1/2} \mathbf{U}_n^T \mathbf{H}(1) \mathbf{V}_n \mathbf{S}_n^{-1/2}, \\ \hat{\mathbf{B}} &= \mathbf{S}_n^{1/2} \mathbf{V}_n^T \mathbf{E}_r, \qquad \hat{\mathbf{C}} = \mathbf{E}_p^T \mathbf{U}_n \mathbf{S}_n^{1/2}, \end{aligned} \quad (6)$$

where the matrices $\hat{\mathbf{A}}$, $\hat{\mathbf{B}}$ and $\hat{\mathbf{C}}$ are estimated quantities, the matrices $\mathbf{S}_n$, $\mathbf{U}_n$, $\mathbf{V}_n$ are obtained by Singular Value Decomposition of the Hankel matrix $\mathbf{H}(0)$, taking into account n significant results. Auxiliary matrices $\mathbf{E}_r$ and $\mathbf{E}_p^T$ contain an appropriate number of identity and zero matrices of order p: $\mathbf{E}_r = [\mathbf{I}_p \mathbf{O}_p \ldots \mathbf{O}_p]$, $\mathbf{E}_p^T = [\mathbf{I}_p \mathbf{O}_p \ldots \mathbf{O}_p]$. An eigenvalue decomposition of the state matrix:

$$\hat{\mathbf{A}}\Phi = \Phi\Lambda, \quad (7)$$

produces a diagonal eigenvalue matrix Λ and a corresponding eigenvector matrix Φ. The mode shapes vectors are the columns of the output matrix defined in modal coordinates $\hat{\mathbf{C}}_m = \hat{\mathbf{C}}\Phi$.

Following the algorithm, ERA belongs to the group of experimental modal analysis in time domain. It uses impulse or free decay responses of the identified system, produced by a dedicated impact excitation, initial condition or sudden interruption of running excitation, e.g., [21]. However, in the light of practical research conclusions, the method is also applicable to ambient vibration signals supplemented by immediate excitation, e.g., [22, 23].

2.2.2. Natural Excitation with ERA (NExT-ERA)

The NExT serves as a tool that converts ambient signals into inputs suitable for experimental modal analysis methods [24]. The combination of NExT and ERA is frequently employed and referred as NExT-ERA technique. Using the NExT, the measured ambient structural response can be transformed into the deterministic form, i.e., the correlation functions of decay character, which corresponds to the free or impulse responses and can be used as an input for the ERA. The cross-correlation function gauges the similarity between two signals in relation to the relative time shift τ between them. It can be interpreted as an estimate of the correlation between two stationary random sequences x_k and y_k

$$R_{x_k, y_k}(\tau) = E[x_{k+\tau} y_k]. \quad (8)$$

For sampled time responses of two output coordinates between two sensors i_1 and i_2, the normalized correlation function is

2

Bull. Pol. Acad. Sci. Tech. Sci., vol. 73, no. 1, p. e152217, 2025

computed as:

$$R_{x_k, y_k}(\tau) = R_{x_{i_1}, y_{i_2}}(k\Delta t) = \frac{1}{N}\sum_{n=0}^{N-\tau-1} x_{i_1,n} y_{i_2, n-\tau}. \quad (9)$$

Once the cross-correlation functions for each measurement point are acquired, the Markov parameters $\mathbf{Y}_k$ in the Hankel matrix $\mathbf{H}(k-1)$ are substituted with the cross-correlation functions R_{x_k, y_k}. This definition of the Hankel matrix allows for the continuation of the modal identification process, following the scheme of the ERA method.

2.2.3. Covariance Driven Stochastic Subspace Identification (SSI-Cov)

The Covariance Driven Stochastic Subspace Identification (SSI-Cov) method was used in system identification [25]. It is classified as an output-only, parametric operational modal analysis in time domain. The basic principle of the SSI-Cov involves the determination of a state-space model of order n, based on the measured ambient vibration responses. The excitation effect is considered a zero-mean white noise, represented by the disturbance vectors $\mathbf{w}_k \in \mathbb{R}^{n\times 1}$ and $\mathbf{v}_k \in \mathbb{R}^{p\times 1}$. Thus, the discrete-time stochastic space-state model is defined by system of equations

$$\begin{aligned} \mathbf{x}_{k+1} &= \mathbf{A}\mathbf{x}_k + \mathbf{w}_k, \\ \mathbf{y}_k &= \mathbf{C}\mathbf{x}_k + \mathbf{v}_k. \end{aligned} \quad (10)$$

The method starts with formulation of data matrices from measured Markov parameters $\mathbf{Y}_k$ [19] and computation of output correlations $\hat{\mathbf{R}}_s$

$$\hat{\mathbf{R}}_s = \frac{1}{N-s}\mathbf{Y}_{(1:N-s)}\mathbf{Y}_{(s:N)}^T, \quad (11)$$

where $\mathbf{Y}_{(1:N-s)}$ is obtained from data matrix $\mathbf{Y}_{(1:N)}$ by removing the last s samples, while $\mathbf{Y}_{(s:N)}$ by removing the first s samples. $\hat{\mathbf{R}}_s$ denotes the unbiased estimate of the correlation matrix at time lag s based on a finite number of data, p is a number of sensors considered and N is a total number of samples in response signal.

The estimated correlation at different time lags is gathered into the block Toeplitz matrix $\mathbf{T}_{1|s} \in \mathbb{R}^{ps \times ps}$

$$\mathbf{T}_{1|s} = \begin{bmatrix} \hat{\mathbf{R}}_s & \hat{\mathbf{R}}_{s-1} & \cdots & \hat{\mathbf{R}}_1 \\ \hat{\mathbf{R}}_{s+1} & \hat{\mathbf{R}}_s & \cdots & \hat{\mathbf{R}}_2 \\ \vdots & \vdots & \ddots & \vdots \\ \hat{\mathbf{R}}_{2s-1} & \hat{\mathbf{R}}_{2s-2} & \cdots & \hat{\mathbf{R}}_s \end{bmatrix}. \quad (12)$$

Factorization of Toeplitz matrix using Singular Value Decomposition (SVD)

$$\mathbf{T}_{1|s} = \mathbf{U}\mathbf{S}\mathbf{V}^T = \begin{bmatrix} \mathbf{U}_n & \hat{\mathbf{U}} \end{bmatrix} \begin{bmatrix} \mathbf{S}_n & \mathbf{0} \\ \mathbf{0} & \hat{\mathbf{S}} \end{bmatrix} \begin{bmatrix} \mathbf{V}_n^T \\ \hat{\mathbf{V}}^T \end{bmatrix} \quad (13)$$

and omitting nonsignificant singular values and corresponding vectors yield

$$\mathbf{T}_{1|s} = \mathbf{P}_s\mathbf{\Gamma}_s = \mathbf{U}_n\mathbf{S}_n\mathbf{V}_n^T. \quad (14)$$

Matrices $\mathbf{P}_s$ and $\mathbf{\Gamma}_s$ are consecutively observability and reversed controllability matrices. Their definition

$$\mathbf{P}_s = \mathbf{U}_n\mathbf{S}_n^{1/2}, \qquad \mathbf{\Gamma}_s = \mathbf{S}_n^{1/2}\mathbf{V}_n^T. \quad (15)$$

allows us to estimate output matrix $\mathbf{C}$ as first n columns of matrix $\mathbf{P}_s$ and state matrix $\mathbf{A}$ as

$$\mathbf{A} = \mathbf{P}^{\uparrow\dagger}\mathbf{P}^{\downarrow}, \quad (16)$$

where $\dagger$ denotes the pseudo-inverse of a matrix. Matrices $\mathbf{P}^{\uparrow}$ and $\mathbf{P}^{\downarrow}$ are defined as shifted matrices of observability matrix $\mathbf{P}$ obtained by removing the last and the first p rows, respectively. Natural frequencies are identified by solving eigenvalue problem of the state matrix $\mathbf{A}$. Corresponding mode shapes are computed using eigenvectors and output matrix $\mathbf{C}$.

2.3. Considered structures

2.3.1. Laboratory beam

The steel cantilever beam with dimensions of $2\times 0.06\times 0.01$ [m] was under investigation. The beam was clamped in hydraulic clams of Zwick/Roell Z400 strength machine to fulfil fixation condition. Its vibrations in horizontal direction (more compliant) were measured in eight sections (sensors P1–P8) spaced in the uniform distances (Fig. 1). A 16-bit HDM QuantumX acquisition system (Hottinger Baldwin Messtechnik GmbH, Darmstadt, Germany) was used, together with one-dimensional piezoelectric accelerometers Isotron Endevco 7752-1000 (PCB Piezotronics Inc., Depew, NY, USA) with a voltage sensitivity of 1 V/g ($\pm 20\%$) and an amplitude response of $0.02 \div 500$ Hz ($\pm 5\%$).

Tests were performed in two beam states: before and after damage was introduced. The damage was induced in the form of 5 mm width saw cut located at $x_d = 1.44$ m from the support, between points P3 and P4 (Fig. 1), with the depth of 0.5 cm. Ambient excitation was considered to provide data for SSI-Cov and NExT-ERA modal identification algorithms. Thirty-minutes signals were collected with a sampling frequency of 200 Hz, giving signals with 360 000 samples. For the ERA technique short-lasting decaying signals were collected after
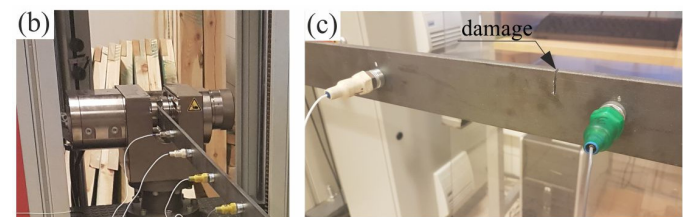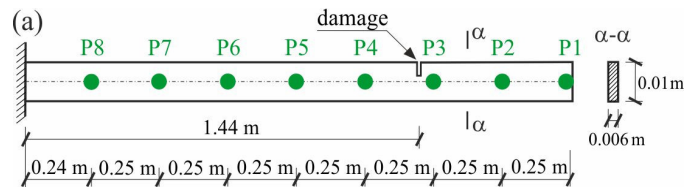

Fig. 1. The laboratory beam: (a) the scheme with the sensors arrangement; (b) the anchor area; (c) the damage area

application of initial displacement at the free end of the beam (ERA-b case), which is in line with the method definition, however difficult to apply in cases of real constructions. Due to this practical limitation, a hit in the model support (machine clamps) was introduced as the second scenario of free-vibration inducing (ERA-m case), mimicking structural excitation caused by ground vibrations.

Assumptions concerning baseline mode shape. The following four possibilities were considered:

- Real measurement of the undamaged structure (RM).
- Analytical function (AF).
  The general free vibration response uniform modal function W is derived from Euler-Bernoulli theoretical representation of a prismatic cantilever beam with length L [26]. The coefficient β changes for each mode shape j.

$$
\begin{aligned}
W^j(x) &= \frac{a-b}{\sinh\beta_j L + \sin\beta_j L}, \\
a &= (\sinh\beta_j L + \sin\beta_j L)(\cosh\beta_j x - \cos\beta_j x), \\
b &= (\cosh\beta_j L + \cos\beta_j L)(\sinh\beta_j x - \sin\beta_j x).
\end{aligned}
\tag{17}
$$

- Finite Element Method (FEM) model.
  The numerical model of the analyzed beam was created using SIMULIA Abaqus software and FEM. An 8-node linear brick element with three transitional degrees of freedom at each node (element C3D8) was selected to generate a mesh grid size of 0.0025 [m]. The material properties were assumed based on standard characteristics of steel, which are: elastic modulus $E = 210$ GPa, Poisson's ratio $\nu = 0.3$, material density $\rho = 7850$ kg/m^3. The first four natural frequencies of the beam were identified from measurements and they were similar to the calculated values, in the undamaged case of the beam.

- Approximation of current mode shape (GSM).
  Gapped smoothing method (GSM) was utilized, which assumes that the mode shape of a healthy beam exhibits a smooth curve and it can be approximated by a polynomial function $\Phi_j(z)$ [27, 28]:

$$
\Phi_j(z) = \sum_{l=0}^{j+1} c_l z^l,
\tag{18}
$$

where z is a distance coordinate of sensor location and j being number of bending mode shape. The parameters c_l are calculated using the least squares method.

2.3.2. Historic masonry lighthouse

The lighthouse, constructed in 1894, sits approximately 40 m from the bank of the Dead Vistula River channel in the Port of Gdańsk, across the Westerplatte Peninsula. Rising to a total height of 27.3 meters, the tower is a monumental stone and masonry-build structure. A brief description of the structure was presented in [23], following an in-situ inventory and examination of technical documentation. During the World War II, the upper part of the structure was damaged by a cannon [29]. The shot made a vast breach in the tower wall, however the tower remained

standing due to its strong internal construction (central core + winding stone staircase). It was repaired between the 1940s and 1950s using new brick material (Fig. 2). Nowadays the technical condition of the structure is recognized as good, with no visible cracks indicating structural damage.
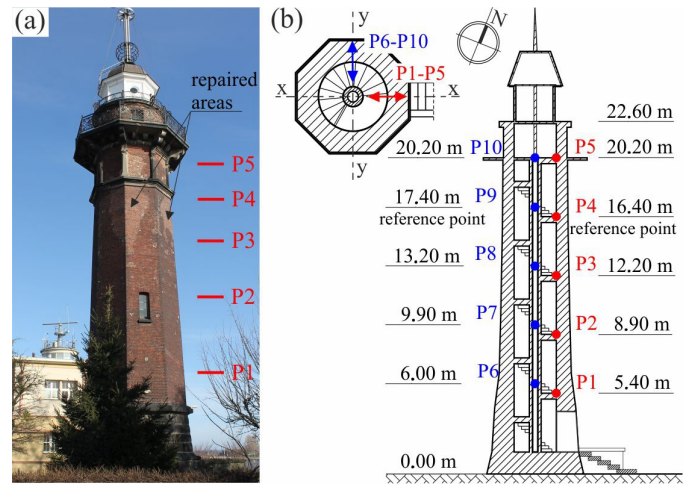

Fig. 2. (a) the lighthouse; (b) sensors arrangement and directions of measurements

An opportunity arose to capture amplified structural vibrations during the operation of a peel hammer located 40 m from the tower [23]. Thus, both ambient vibration signals (SA) and forced vibration signals (SH) amplified by the hammering were gathered and analyzed. Sensors (measuring points) were positioned along two vertical axes and affixed to the stairs near the walls (points P1–P5 and points P6–P10 according to the Fig. 2). They collected horizontal accelerations in two perpendicular directions to identify bending modes in two principal directions. It was presumed that one of these directions aligned with stone-made, external stairs integrated into the tower. Moreover, considering the stair's orientation toward the river, excitation from water waving originating in that direction - could influence the principal direction of vibrations in this nearly symmetric structure.

The same equipment was used for laboratory beam measurements. Due to channels limitations, four series of measurements were carried out with the reference points P4 and P9. The duration of SA signals was set to 1200 s, while the length of SH signals varied depending on duration of sheet pile driving (from several dozen seconds to several minutes). The sampling frequency was 200 Hz, with the vibratory hammer operating at approximately 34 Hz. The collected signals allowed the application of three mentioned operational modal analysis techniques for system identification. Both SA and SH signals were considered in the NExT-ERA and SSI-Cov techniques, while short-lasting parts of signals of decaying character were selected from both kinds of vibrations for ERA. These segments of structural response were induced by water waves generated by boats floating on the river, so the impulses transmitted through the foundations.

4

Bull. Pol. Acad. Sci. Tech. Sci., vol. 73, no. 1, p. e152217, 2025

Assumptions concerning baseline mode shape. In this case two possibilities were utilized. The GSM described in Section 2.3.1 and FEM model-based mode shape. The FEM model of the lighthouse is described in [23].

3. RESULTS AND DISCUSSION

First bending mode shapes of both structures were considered. Multiple realizations of the ERA and NExT-ERA algorithms were made, considering different orders of the systems and a few sections of vibration signal of decaying character, in the case of ERA. This provided sets of variants of the mode shape obtained by the two techniques. The SSI technique produces one modal result, based on the whole measured vibration signals.

3.1. Laboratory beam

The mode shape identified with the four techniques is presented in Fig. 3. The presence of damage is marked by a local breakdown of the mode. The single result for SSI-Cov technique is presented and multiple outputs for other methods, resulting in a thicker line of the mode shape plot, which is actually a composition of several lines of different solutions. The most significant discrepancies occur in the ERA-m case.
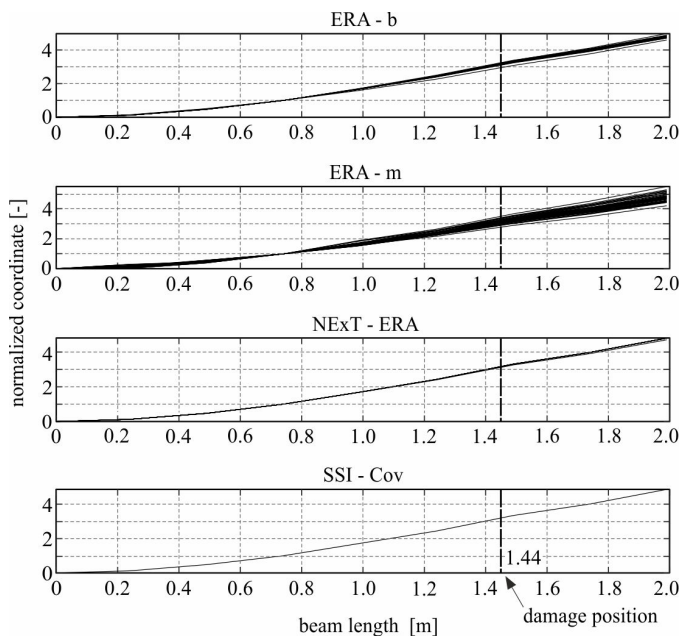
Fig. 3. The first bending mode shape of the beam, identified with the four approaches

The Z indices values obtained for different modal identification techniques and different strategies of baseline data determination are presented in Figs. 4–7. The horizontal axis in the graphs represents P1-P8 sections of the beam, while the vertical axis refers to various variants of the mode shape. The colour of each cell indicates the Z index value, with the reference to the legend placed on the right of each plot. The upper limit of the plot scale is set to 2.5, as no values greater than this were obtained.
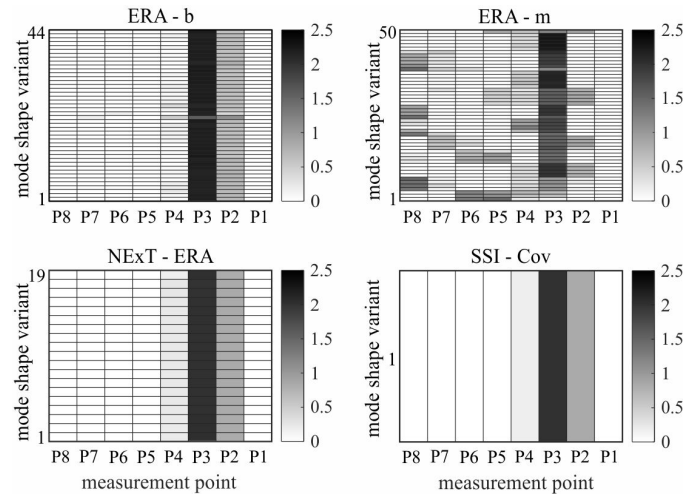

Fig. 4. Z indices values for beam for FEM baseline data and mode shape from the given MID method
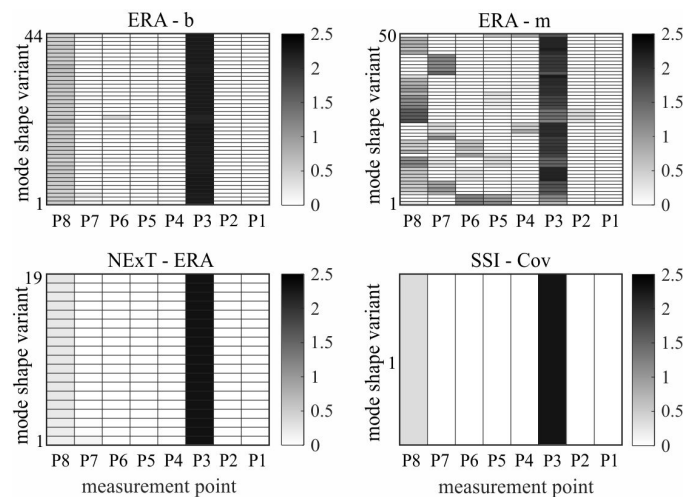

Fig. 5. Z indices values for beam for GSM baseline data and mode shape from the given MID method
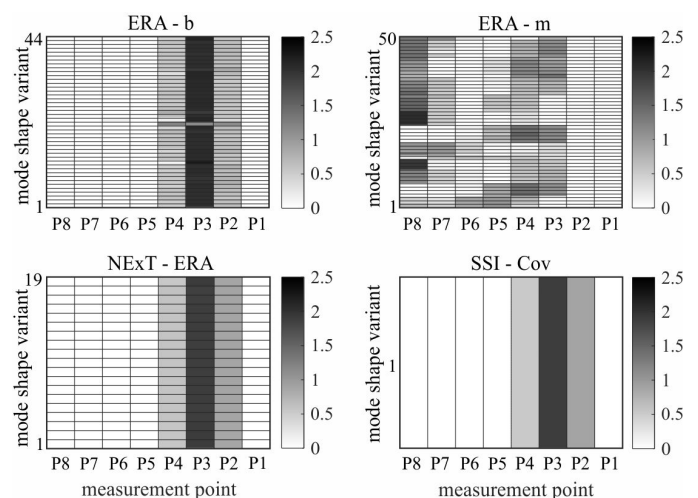

Fig. 6. Z indices values for beam for RM baseline data and mode shape from the given MID method

Bull. Pol. Acad. Sci. Tech. Sci., vol. 73, no. 1, p. e152217, 2025
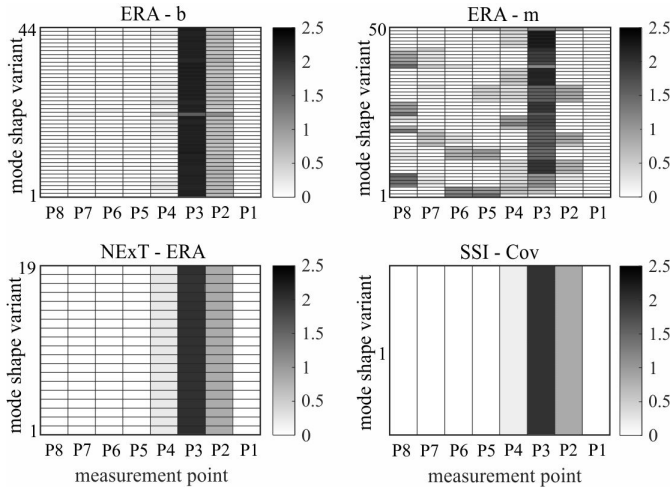
5

Fig. 7. Z indices values for beam for AF baseline data and mode shape from the given MID method

In the case of ERA, the effectiveness of damage indication depends largely on the applied method of vibration excitation. In the ERA-b case, the discrepancy of the identified mode shape is relatively small (see Fig. 3), which results in the good stability of damage location indication, similar to those obtained with the NEXT-ERA and SSI-Cov methods. This is due to the fact that this type of excitation (initial condition) produces a good quality response signals, which satisfy directly the method assumptions. However, such excitation is difficult to implement in the case of real structures of considerable size (e.g., bridges and towers), because it requires dedicated initial excitation (e.g., tugging, swaying, dropping the weight, etc.) or applying external forces by the use of exciters that have force-controlling instrumentation. In the ERA-m case, a greater discrepancy in the identified mode shapes occurs (see Fig. 3), which results in lowering of the damage location indication efficacy.

This is particularly in the case of RM-baseline strategy (see Fig. 6), because both 'undamaged' and 'damaged' mode shapes are burdened with discrepancies. In the case of FEM, GSM and AF, the baseline mode shape is unambiguously defined, which positively affects the effectiveness of damage indication. Most often section P3 is indicated, which is the correct result. However there are also indicators to P1 section and also there is no damage localization, with low Z index values for all eight considered sections of the beam.

The above observations are in accordance with the previous works [22, 23], which demonstrated the possibility of applying the ERA to ambient data, however multiple realizations using different parts of response signals are required.

All methods of baseline data determination led to similar effectiveness in damage detection in case of SSI-Cov and NExT-ERA applying. However, the results obtained using the GSM method are the most precise (Fig. 5) – there is the most clear indication at the P3 section, situated next to the damage, where the Z index exceeds the value of 2. In the other three kinds of baseline data the damage localization is more blurry, demonstrating some probability of the damage situated in neighbouring sections P2 and P4.

The outstanding positive results obtained using GSM are particularly satisfactory because this is the simplest method, easily applicable in practical cases of real structures, where neither reference data are available nor FEM model can be easily built. This method appears to be the most promising for indicating damage in the next case, that of the lighthouse.

3.2. Masonry lighthouse

The first mode shape of the structure, identified with ERA and NExT-ERA is presented in [23]. In the present study multiple realizations of the techniques are made, thus sets of solutions exist when considering ERA and NExT-ERA, similarly like in the previous case, of the laboratory beam. The SSI-Cov technique produces a single result.

The Z indices values obtained for the lighthouse are depicted in Figs. 8–11, organized similarly to Figs. 4–7. Three modal identification techniques and two baseline data determination strategies were considered.

The parts of the walls rebuilt in the tower are visible between height levels P3–P4 and P8–P9 (see Fig. 2). Thus, an increase in Z value is expected for these section, which is indeed observed in most considered variants of the analysis. The indication was particularly clear when NExT-ERA and SSI-Cov techniques were used. The Z values obtained from the ERA-based modal data are blurred, similarly to the beam case, where ERA-m simulated excitation coming from the ground. That means, once again, that the existence of different variants of the ERA solution imposes considerable impact on the damage detection possibility – not
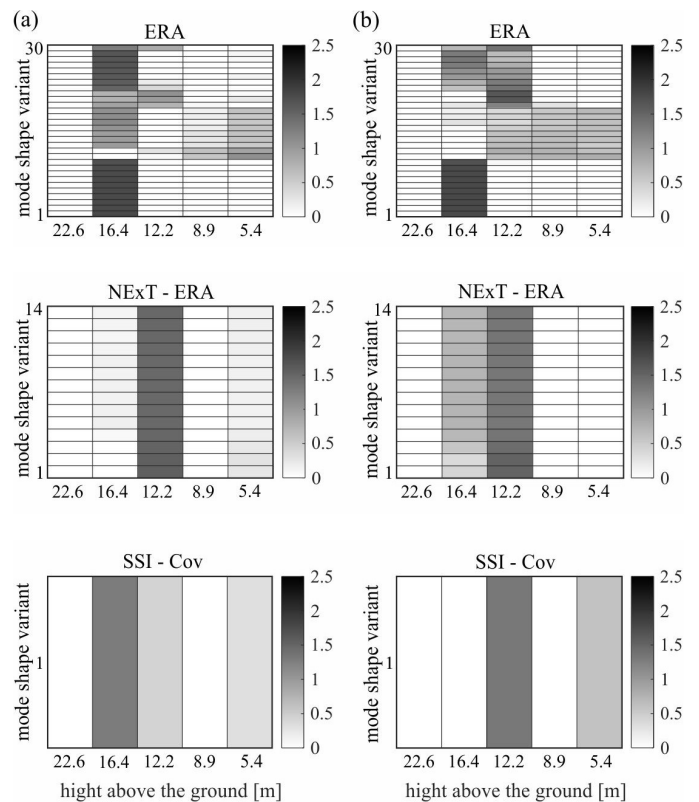

Fig. 8. Z indices values for lighthouse, input: SA signals, points P1-P5 and top of the masonry wall, baseline data from (a) FEM; (b) GSM

6

Bull. Pol. Acad. Sci. Tech. Sci., vol. 73, no. 1, p. e152217, 2025

Efficacy of modal curvature damage detection in various pre-damage data assumptions and modal identification techniques
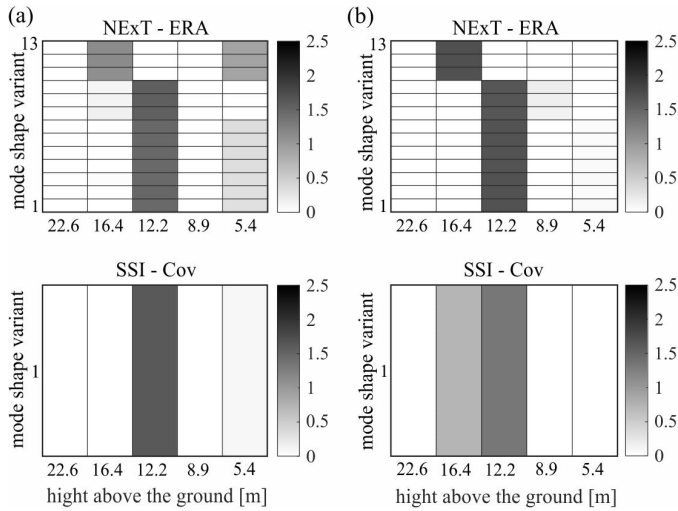

Fig. 9. Z indices for lighthouse, input: SA+SH signals, points P1-P5 and top of the masonry wall, baseline data from (a) FEM; (b) GSM
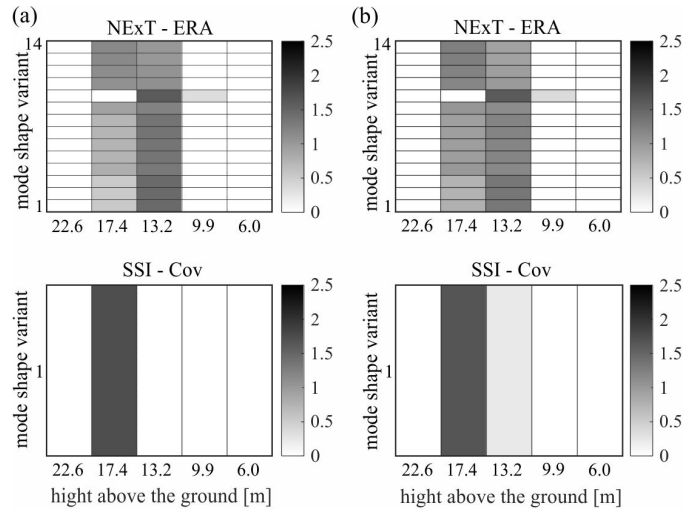

Fig. 11. Z indices for lighthouse, input: SA+SH signals, points P6-P10 and top of the masonry wall, baseline data from (a) FEM; (b) GSM
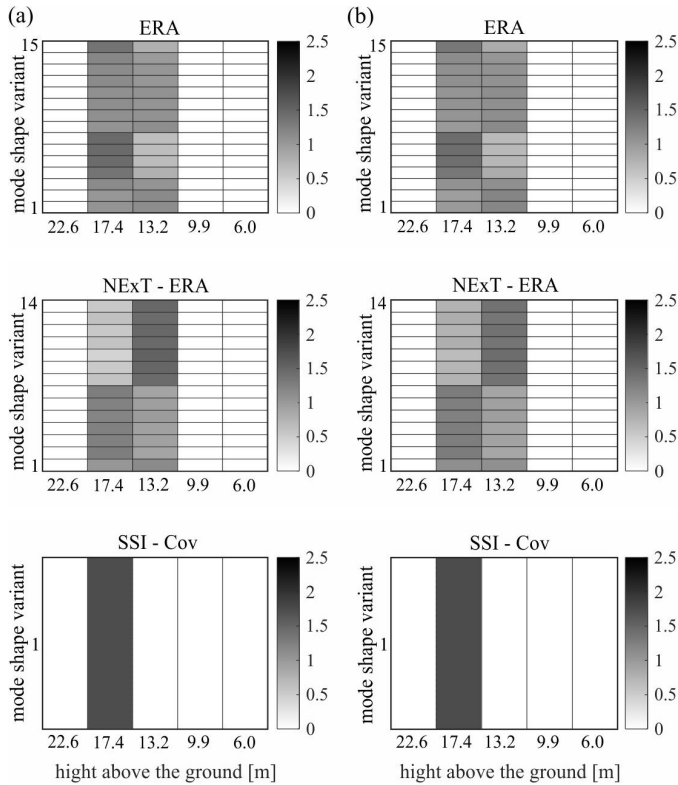
4. CONCLUSIONS

The research proves that the efficiency of modal curvature method may vary depending on modal identification technique used to obtain mode shapes. The ERA results should be considered carefully and, preferably, a set of results should be included in the damage localization, to avoid false results. The other two MID methods produce more reliable data for this method of damage detection. This conclusion is drawn from the analysis of both cases analysis, laboratory beam and historic stone-masonry tower.

In the beam case, using the GSM for baseline data definition led to the highest accuracy of the damage localization. In the lighthouse case, the two considered methods of baseline data possessing yield comparable results. These results allow us to conclude that the GSM is the most convenient one, as it leads to reliable results and is easy in application.

To summarize, the modal curvature method, pioneer one in damage localization, provides reliable results and remains applicable in practical cases, although modern methods, such as machine learning have been proposed [30].

Fig. 10. Z indices values for lighthouse, input: SA signals, points P6-P10 and top of the masonry wall, baseline data from (a) FEM; (b) GSM

ACKNOWLEDGEMENTS

every ERA solution leads to proper damage location. That happened for ERA solutions in variants no. 11–20 for points P1–P5, ambient excitation, see Fig. 8.

Comparing the effectiveness of damage detection regarding possession of reference data, the results obtained based on FEM and GSM are comparable. That means that the GSM method, which is practically the easiest to apply, is reliable and can be used in practical cases of damage detection.

REFERENCES

[1] C.P. Fritzen, "Vibration-based structural health monitoring – concepts and applications," *Key Eng. Mater.*, vol. 293–294, p. 3–20, 2005.

[2] S.S. Saidin, S.A. Kudus, A. Jamadin, M.A. Anuar, N.M. Amin, A.B.Z. Ya, and K. Sugiura, "Vibration-based approach for structural health monitoring of ultra-high-performance concrete bridge," *Case Stud. Constr. Mater.*, vol. 18, p. e01752, 2023, doi: 10.1016/j.cscm.2022.e01752.

[3] J. Zhang, C.-X. Qu, T.-H. Yi, H.-N. Li, Y.-F. Wang, and X.-D. Mei, "Detecting deck damage in concrete box girder bridges using mode shapes constructed from a moving vehicle," *Eng. Struct.*, vol. 305, p. 117726, 2024, doi: 10.1016/j.engstruct.2024.117726.

[4] S. Carbonari, F. Dezi, D. Arezzo, and F. Gara, "A methodology for the identification of physical parameters of soil-foundation-bridge pier systems from identified state-space models," *Eng. Struct.*, vol. 255, p. 113944, 2022, doi: 10.1016/j.engstruct.2022.113944.

[5] J.M.W. Brownjohn, A. Raby, J. Bassitt, A. Antonini, E. Hudson, and P. Dobson, "Experimental modal analysis of british rock lighthouses," *Mar. Struct.*, vol. 62, pp. 1–22, 2018, doi: 10.1016/j.marstruc.2018.07.001.

[6] R.M. Azzara, M. Girardi, V. Iafolla, D.M. Lucchesi, C. Padovani, and D. Pellegrini, "Ambient vibrations of age-old masonry towers: Results of long-term dynamic monitoring in the historic centre of lucca," *Int. J. Archit. Herit.*, vol. 15, no. 1, pp. 5–21, 2021.

[7] A.R. Carmelo Gentile and A. Saisi, "Continuous dynamic monitoring to enhance the knowledge of a historic bell-tower," *Int. J. Archit. Herit.*, vol. 13, no. 7, pp. 992–1004, 2019.

[8] K. Wilde and M. Rucka, "Ultrasound monitoring for evaluation of damage in reinforced concrete," *Bull. Pol. Acad. Sci. Tech. Sci.*, vol. 63, no. 1, pp. 65–75, 2015, doi: 10.1515/bpasts-2015-0008.

[9] A. Knitter-Piątkowska, O. Kawa, and M.J. Guminiak, "Damage localization in truss girders by an application of the discrete wavelet transform," *Bull. Pol. Acad. Sci. Tech. Sci.*, vol. 71, no. 1, p. e144581, 2023, doi: 10.24425/bpasts.2023.144581.

[10] L. Hadjileontiadis, E. Douka, and A. Trochidis, "Fractal dimension analysis for crack identification in beam structures," *Mech. Syst. Signal Process.*, vol. 19, no. 3, pp. 659–674, 2005, doi: 10.1016/j.ymssp.2004.03.005.

[11] A. Pandey, M. Biswas, and M. Samman, "Damage detection from changes in curvature mode shapes," *J. Sound Vibr.*, vol. 145, no. 2, pp. 321–332, 1991, doi: 10.1016/0022-460X(91)90595-B.

[12] M. Abdel Wahab and G. De Roeck, "Damage detection in bridges using modal curvatures: Application to a real damage scenario," *J. Sound Vibr.*, vol. 226, no. 2, pp. 217–235, 1999, doi: 10.1006/jsvi.1999.2295.

[13] R. Taghipour, M.R. Nashta, M. Bozorgnasab, and H. Mirgolbabaei, "A new index for damage identification in beam structures based on modal parameters," *Arch. Mech. Eng.*, vol. 68, no. 4, pp. 375–394, 2021, doi: 10.24425/ame.2021.138397.

[14] L. Wang, R. Chen, L. Dai, K. Huang, J. Zhang, and C. Tang, "A detection method integrating modal deflection curvature difference and natural frequency for structural stiffness degradation," *Eng. Fail. Anal.*, vol. 141, p. 106637, 2022, doi: 10.1016/j.engfailanal.2022.106637.

[15] Y. Jiang, J. Sun, Q. Lin, and J. Xiang, "A two-stage method to detect damages in aluminum plates using curvature modal shape subtraction indicator and particle swarm optimization," *Thin-Walled Struct.*, vol. 185, p. 110560, 2023, doi: 10.1016/j.tws.2023.110560.

[16] A. Anwar and A. Abd Elwaly, "Modal displacement vs curvature functions as damage identifier for masonry structures," *Alex. Eng. J.*, vol. 68, pp. 527–538, 2023, doi: 10.1016/j.aej.2023.01.042.

[17] D.H. Nguyen, Q.B. Nguyen, T. Bui-Tien, G. De Roeck, and M. Abdel Wahab, "Damage detection in girder bridges using modal curvatures gapped smoothing method and convolutional neural network: Application to bo nghi bridge," *Theor. Appl. Fract. Mech.*, vol. 109, p. 102728, 2020, doi: 10.1016/j.tafmec.2020.102728.

[18] B.L. Ho and R.E. Kalman, "Effective construction of linear, state-variable models from input/output functions," *Regelungstechnik*, vol. 14, no. 12, 1966.

[19] J.-N. Juang and R. Pappa, "An eigensystem realization algorithm for modal parameter identification and model reduction," *J. Guid. Control Dyn.*, vol. 8, pp. 620–627, 1985.

[20] J.-N. Juang, *Applied System Identification*. Englewood Clifs, New York, USA: Prentice-Hall PTR, 1994.

[21] M. Szafrański, "A dynamic vehicle-bridge model based on the modal identification results of an existing en57 train and bridge spans with non-ballasted tracks," *Mech. Syst. Signal Process.*, vol. 146, p. 107039, 2021, doi: 10.1016/j.ymssp.2020.10703.

[22] A. Tomaszewska and M. Szafrański, "Study on applicability of two modal identification techniques in irrelevant cases," *Arch. Civ. Mech. Eng.*, vol. 20, no. 13, p. 13, 2020, doi: 10.1007/s43452-020-0014-8.

[23] A. Tomaszewska, M. Drozdowska, and M. Szafrański, "Material parameters identification of historic lighthouse based on operational modal analysis," *Materials*, vol. 13, no. 17, p. 3814, 2020, doi: 10.3390/ma13173814.

[24] G.H. James III, T.G. Carne, and J.P. Lauffer, "The natural excitation technique (next) for modal parameter extraction from operating wind turbines," *NASA STI/Recon Technical Report N*, vol. 93, p. 28603, 1993.

[25] P. van Overschee and B. De Moor, "Subspace algorithms for the stochastic identification problem," *Automatica*, vol. 29, pp. 649–660, 1993, doi: 10.1016/0005-1098(93)90061-W.

[26] W.J. Bottega, *Engineering vibrations*. CRC Press, 2014.

[27] C.P. Ratcliffe and W.J. Bagaria, "Vibration technique for locating delamination in a composite beam," *AIAA J.*, vol. 36, no. 6, pp. 1074–1077, 1998.

[28] S. Rucevskis, R. Janeliukstis, P. Akishin, and A. Chate, "Mode shape-based damage detection in plate structure without baseline data," *Struct. Control Health Monit.*, vol. 23, no. 9, pp. 1180–1193, 2016.

[29] "Lighthouse gdańsk nowy port." [Online]. Available: http://www.latarnia.gda.pl/english/

[30] A. Anjum, M. Hrairi, A. Aabid, N. Yatim, and M. Ali, "Damage detection in concrete structures with impedance data and machine learning," *Bull. Pol. Acad. Sci. Tech. Sci.*, vol. 72, p. e149178, 2024, doi: 10.24425/bpasts.2024.149178.

8

Bull. Pol. Acad. Sci. Tech. Sci., vol. 73, no. 1, p. e152217, 2025